**Original**

# Comparison of the wound-healing efficacy of gelatin sponge dressings and that of artificial dermis using atelocollagen in a rat cranial periosteal defect model

Yasuyuki ASADA[1)], Shinya KOSHINUMA[1)], Masaki MIKAMI[2)], Yuuki SHIRAI[1)],
Yoshisato MACHIDA[1)], Takahisa NAKAYAMA[3)], Ryoji KUSHIMA[3)],
Gaku YAMAMOTO[1)] and Ken-ichi MUKAISHO[3)]

[1)]*Department of Oral and Maxillofacial Surgery, Shiga University of Medical Science, Seta-Tsukinowa-Cho, Otsu, Shiga 520-2192, Japan*
[2)]*Department of Oral and Maxillofacial Surgery, Kyoto Second Red Cross Hospital, 355-5 Haruobi-cho, Kamigyo-ku, Kyoto 602-8026, Japan*
[3)]*Division of Human Pathology, Shiga University of Medical Science, Seta-Tsukinowa-Cho, Otsu, Shiga 520-2192, Japan*

**Abstract:** In oral surgery, tissue loss may occur in some cases, resulting in bone exposure and subsequent wound infection and possible scar formation during secondary healing. In this study, Terudermis® Artificial Dermis (AD-T), a dermal defect graft made from processed bovine dermis collagen and gelatin sponge (GS) were used as dressings on 100-mm$^2$ wounds with exposed bone on the heads of rats. For the control group, the wound was left exposed. The wound-healing efficacy of the treatment was compared macroscopically and histologically among the three groups at 1, 2, and 4 weeks after surgery. Complete wound healing was achieved faster in the AD-T group than in the GS group, and osteoblasts appeared on the bone surface, indicating accelerated bone remodeling. Furthermore, in the AD-T group, there was an increased production of newly formed blood vessels, fibroblasts and osteoblasts positive for anti-cortactin antibodies, which are believed to contribute to wound healing. Our findings suggest that AD-T is better than GS as a wound dressing material.
**Key words:** artificial dermis, atelocollagen, cortactin, dressing material, wound healing

## Introduction

In oral surgery, especially in tumor resection, some procedures may result in a loss of soft tissue, which inevitably leads to exposure of the bone underneath the soft tissue [1]. If the extent of bone exposure is small, the condition can be managed by simply suturing or by leaving the wound open to attempt a secondary healing [2]. However, if the area of the defect is large and the bone is extensively exposed, closure needs to be done by filling the defect through immediate reconstruction using large flaps, such as free flaps, pedicled flaps, or local flaps [3, 4]. Conventionally, palatal mucosa trans-

plantation and wound dressing with various artificial materials have been carried out to treat medium-sized defects that are difficult to suture but not large enough to require the use of flaps [3–6]. However, mucosal transplantation and skin grafting pose an issue of secondary invasion of the donor site, and the disadvantage of most artificial materials is that they have low biocompatibility [2–6]. In light of the above information, new wound dressings have been actively developed since the early 1980s to promote wound healing [7]. In a previous study, we prepared 100-mm$^2$ wounds with exposed bone surfaces on the heads of rats; the wounds were covered with gelatin sponge (GS; the GS group), PGA sheets with

fibrin glue dressing (PGA-FG; the PGA-FG group), or were left open (the control group); and the healing process of the wound after 2, 4, and 6 weeks was observed macroscopically and microscopically in each group [8]. Our findings showed that wound healing was completed earlier in the GS group than in the other groups [8]. In this study aimed at finding wound dressing materials with a wound-healing effect superior to that of GS, artificial dermis Terudermis® (AD-T, a graft for dermal defects, which is made from processed bovine dermis-derived collagen) was used, and its wound-healing effect was compared to that of GS. We also performed immunohistochemical staining using anti-cortactin antibodies, which have been shown to contribute to wound healing, to clarify the underlying mechanism by which AD-T promotes wound healing [9].

## Materials and Methods

### Animals

Forty-five 10-week-old male Wistar rats (Japan SLC, Inc., Shizuoka, Japan) were used. The rats were classified into three separate groups. The first group consisted of the AD-T group in which Terudermis® (artificial dermis Terudermis, AD-T) was used as a wound dressing; the second group consisted of the GS group in which Spongel® (GS) was used; and the third group consisted of the control group, in which the wound was left open. The three groups were compared on the basis of the wound-healing condition at 1, 2, and 4 weeks after surgery. Each group included 15 rats; five rats were assigned each week.

The rats were kept at the Research Center for Animal Life Science, Shiga University of Medical Science, in an environment maintained at controlled levels of temperature and humidity ($23 \pm 3$°C, $55 \pm 15$%). During the experimental period, the rats were fed with water and food CLEA Rodent Diet CE-2 (CLEA Japan, Inc., Tokyo, Japan) with no restrictions. This study was approved by the Shiga University of Medical Science Ethics Committee on Animal Experimentation (project approval number 2018-6-1) and was conducted in accordance with Shiga University of Medical Science's guidelines pertaining to animal experimentation as well as in accordance with the Act on Welfare and Management of Animals.

### Implant materials

In the AD-T group, the implant material consisted of AD-T (Olympus Terumo Biomaterials, Inc., Tokyo, Japan), which was made from bovine dermis-derived collagen treated with protease for the removal of the telopeptide portions in order to obtain atelocollagen with no

antigenicity.

In the GS group, the implant material consisted of GS (LTL Pharma, Inc., Tokyo, Japan) with an isoelectric point of 4.9 and a weight-average molecular weight of 99 kDa.

In the control group, the skin and periosteum of the head were removed, and a wound with exposed bone surface was created without using any wound dressing.

### Operative procedure

All rats were fasted for 24 h before surgery. Inhalation anesthesia using isoflurane was carried out using an inhalation anesthesia device for small animals (Natsume Seisakusho Co, Ltd., Tokyo, Japan). First, the rats were placed in a plastic anesthesia box, and anesthesia was induced using 5% isoflurane. Next, after confirming that the rats' righting reflex was lost, the rats were moved to a nose cone mask, and anesthesia was maintained with 3% isoflurane containing room air. Subsequently, the parietal region was shaved and disinfected. In the parietal region of all rats, the skin and subcutaneous tissue were incised using a scalpel; a square defect with each side measuring 10 mm was created, and the periosteum was detached using a periosteal elevator in order to expose the bone (Fig. 1).

In the AD-T group, an AD-T measuring $10 \times 10$ mm in size was attached to the wound with exposed bone in the parietal region, and the periphery was sutured with eight sutures, using 5-0 resorbable sutures (BEAR Medic, Corp., Tokyo, Japan) (Fig. 1a). In the GS group, a GS measuring $10 \times 10$ mm in size was placed on the wound with exposed bone in the parietal region (Fig. 1b). We attempted to suture the wound in the GS group as well; however, as the GS is a sponge, it was impossible to suture. In the control group, no wound dressing was used, and the bone surface in the parietal region was left exposed (Fig. 1c).

In the previous studies, the problem was that after surgery, the rats touched the wound with their forefeet, or rubbed it against their cage, and as a result, the wound dressing fell off during the course of the experiment. In this study, for the purpose of analgesia and sedation, medetomidine hydrochloride (0.15 mg/kg), midazolam (2 mg/kg), and butorphanol tartrate (2.5 mg/kg) were diluted in physiological saline and injected intraperitoneally once immediately after surgery. Furthermore, in order to prevent the wound from being touched by other rats, the number of rats per cage was limited to only one. To prevent the infection of the surgical wound, tetracycline hydrochloride (18 mg/day/body weight) mixed with tap water was administered during the 5-day period after surgery.
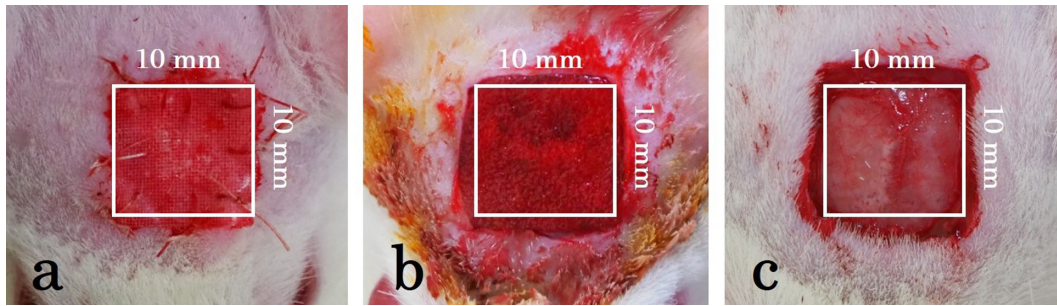
**Fig. 1.** Representative photographs of defects in the skin and cranial periosteum in each group. a) AD-T group, b) GS group, and c) control group. A 100-mm² defect (surrounded by a white square) in the skin and cranial periosteum has been created in the parietal region of the skull of each rat. Thereafter, an AD-T or a GS dressing has been applied for rat cranial periosteal defect repair (a and b). White circles indicate sutures (a). We have only placed the GS in the exposed bony wound, and it has not been sutured or glued (b). The defect is not covered with any dressing materials in the control group (c).
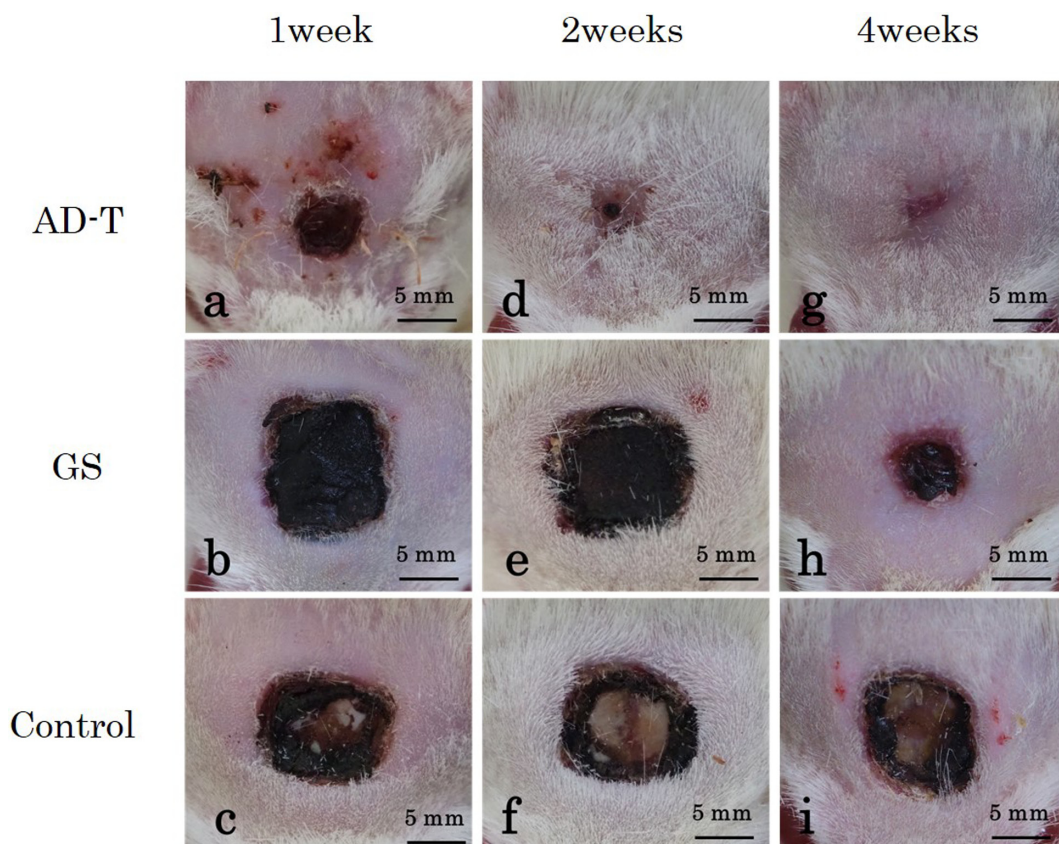


**Fig. 2.** Representative photographs of macroscopic findings. The progression of postsurgical healing in the AD-T (a, d, g), GS (b, e, h), and control groups (c, f, i) observed at 1 week (a–c); 2 weeks (d–f); and 4 weeks (g–i). Complete wound healing has occurred earlier in the AD-T group (at 4 weeks) than in the other groups (g–i).

## Macroscopic findings and measurement of the wound surface defect area

Wounds with exposed bone in each group were photographed (Fig. 2), and using the pictures, the dimensions (area) of skin and periosteal defects in all rats were measured using the software Image J (National Institutes of Health, Bethesda, MA, USA).

## Histological examination

Under general anesthesia using isoflurane, the rats were euthanized by exsanguination, and perfusion fixation was performed using paraformaldehyde 4%. Tissue from the parietal head wound was harvested and was fixed in paraformaldehyde 4% for 2 days. Tissue samples containing bones were decalcified in K-CX solution (Falma Co, Ltd., Tokyo, Japan) for 4 days. The tissues were then divided into four sections by a frontal cut

perpendicular to the wound, embedded in paraffin, and sectioned into 3-$\mu$m-thick slices. Of the four samples (sample #1 to sample #4) shown in Fig. 3, samples #2 and #3 were stained with hematoxylin and eosin (HE) staining. Wound healing and bone remodeling were evaluated on the basis of HE staining.

For immunohistochemical staining, the slices were deparaffinized, immersed in an antigen activator (Nisshin EM Co., Ltd., Tokyo, Japan), and heated at 98°C for 45 min. Endogenous peroxidase was removed, and the slices were reacted overnight at 4°C with anti-cortactin antibody (dilution ratio: 1:100; Abcam, Cambridge, UK, Rabbit. #ab81208) as the primary antibody. The samples were reacted at 37°C for 30 min with the secondary antibody, MAX-PO (MULTI) for rat tissue (Nichirei Bioscience Inc., Tokyo, Japan); and color development was performed using the DAB substrate kit (Nichirei Bioscience Inc.). Subsequently, the cell nuclei were stained with hematoxylin and examined under a microscope.

## Quantitative analysis of cortactin-positive cells

The number of cortactin-positive fibroblasts at 10 randomly selected $100 \times 100\ \mu$m areas was measured under the microscopic image, and the proportion of cortactin-positive fibroblasts to the total number of fibroblasts was determined in each specimen. These were measured using the software Image J (National Institutes of Health).

## Cranial bone thickness

Each rat's cranial bone thickness was measured at 10 randomly selected sites in microscopic images of one specimen. This was performed on two of the four samples (samples #2 and #3) (Fig. 3); thus, measurements were carried out at a total of 20 sites per rat.

## Statistical analyses

One-way analysis of variance and post-hoc pairwise comparisons were performed to analyze the measurements of the wound surface defect areas and the proportion of cortactin-positive fibroblasts among the three groups.

We conducted two types of analysis regarding the rat's cranial bone thickness for the comparison between the AD-T group or the GS group and control group. One is a statistical test about estimation of difference adjusting the specimen in each time point (1, 2, and 4 weeks after surgery); the other is comparisons of straight lines using with the fitting the linear regression model for weeks after surgery. Since 20 sites per rat for cranial bone thickness was measured, the generalized estimating equation (GEE) with identity link function under the assumption
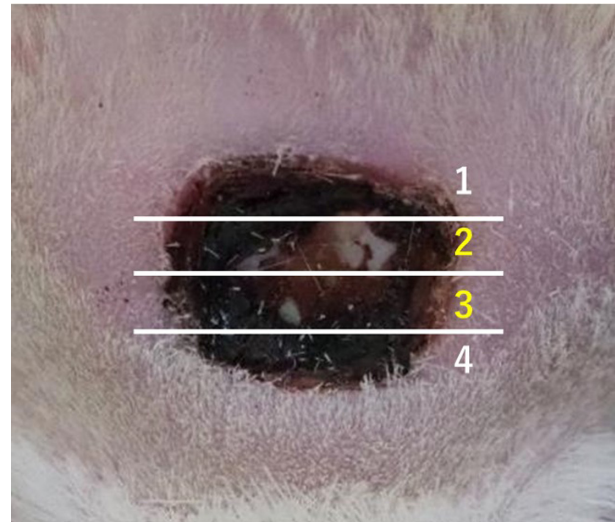


**Fig. 3.** Tissues divided into four by frontal sectioning perpendicular to the wound. To make sections easier for staining of tissue including the bone, the sample has been decalcified in K-CX solution for 4 days, and then the tissue has been divided into four sections by a frontal section perpendicular to the wound and embedded in paraffin. Specimens are prepared with three-micrometer sections.

of normal distribution, which can incorporate the within individual correlation of rat, was applied for the comparison between groups.

All statistical analyses were performed with the use of R (version 4.1.0) and the alpha level was set at 0.05.

## Results

### Macroscopic findings and measurement of the wound surface defect area

Figure 2 shows representative images of wounds in each group at 1, 2, and 4 weeks after surgery. No postoperative dislodgement of AD-T or GS occurred in the present study. At 1 week after surgery, the bone was still exposed in the control group whereas in the AD-T group, the surgical wound had decreased in size and was covered with blood clots (Fig. 2a). In the GS group, the wound was covered with blood clots (Figs. 2b and 2c). Two weeks after surgery, the wounds in the AD-T group showed a further decrease in size and were covered with regenerated epithelium (Fig. 2d). Both in the GS and control groups, the wounds tended to decrease in size; however, in the wounds in the control group, the bone was still exposed and dry, whereas in the GS group, the wounds were covered with blood clots (Figs. 2e and 2f). At 4 weeks after surgery, all rats in the AD-T group showed complete wound closure with skin regeneration (Fig. 2g). In the GS group, the wound showed a further decrease in size and was found to be covered with re-

generated epithelium in one animal (Fig. 2h). In the control group, the area of the wounds remained unchanged and the bone was still exposed (Fig. 2i).

Table 1 shows the results of the wound surface defect area measurements. The data are presented as the mean ± SD. At 1 week after surgery, the defect areas were 35.7 ± 7.7 mm², 86.1 ± 4.1 mm², and 90.7 ± 11.8 mm² in the AD-T group, GS group, and control group, respectively. At 2 weeks after surgery, the defect areas were 9.7 ± 6.9

mm², 79.0 ± 7.3 mm², and 71.5 ± 7.5 mm² in the AD-T group, GS group, and control group, respectively. By 4 weeks after surgery, the defect areas had completely closed for all the rats in the AD-T group, and as a result, the wound area could not be measured. The defect areas in the GS and control groups were 66.5 ± 21.8 mm² and 72.4 ± 6.0 mm², respectively.

At 1 and 2 weeks after surgery, the AD-T and control groups were significantly different (both $P<0.0001$). However, at 4 weeks after surgery, the defect areas had completely closed for all the rats in the AD-T group, and as a result, the wound area could not be measured and no statistical comparison could be performed.

### Histological examination

Figures 4 to 6 show representative microscopic images of the HE-stained tissue sections in each group at 1, 2, and 4 weeks after surgery.

At 1 week after surgery, the AD-T group showed granulation tissue formation composed of numerous fibroblasts and new blood vessels under blood clots (Figs. 4a and 4b). Furthermore, findings confirmed that cubic
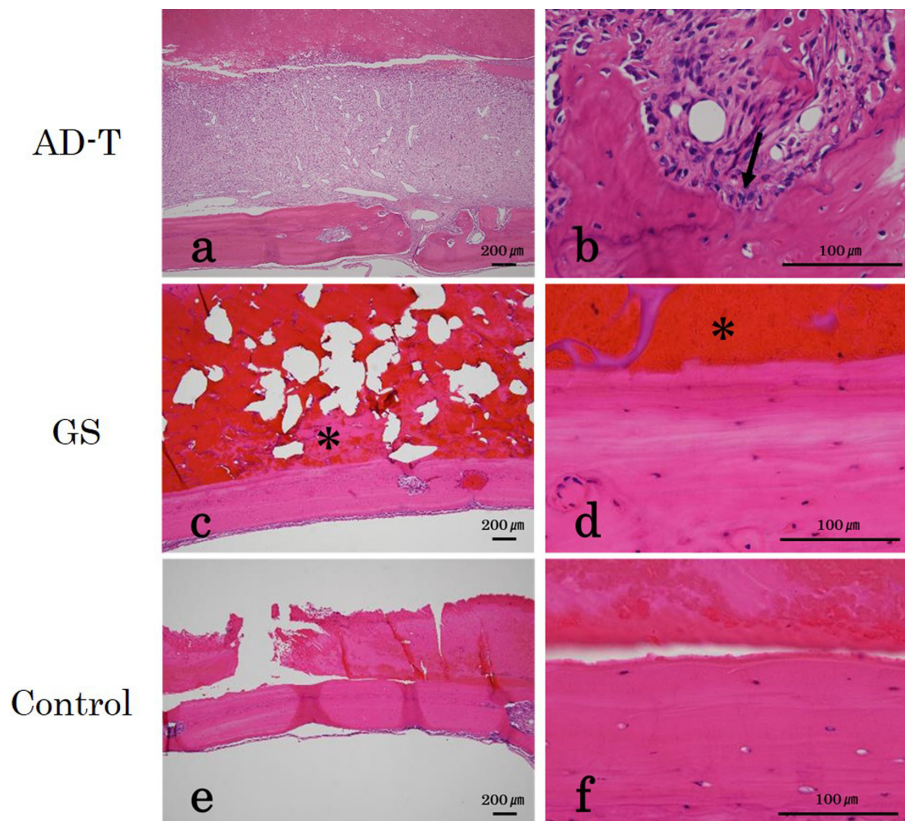
**Table 1.** Summary of measurements of the wound surface defect area

|  | group | mean | SD | *P*-value |
|---|---|---|---|---|
| 1 week after surgery | AD-T | 35.7 | 7.7 | <0.0001 |
|  | GS | 86.1 | 4.1 | 0.3991 |
|  | Control | 90.7 | 11.8 | – |
| 2 weeks after surgery | AD-T | 9.7 | 6.9 | <0.0001 |
|  | GS | 79.0 | 7.3 | 0.1261 |
|  | Control | 71.5 | 7.5 | – |
| 4 weeks after surgery | AD-T | 0 | 0 | No test performed |
|  | GS | 66.5 | 21.8 | 0.5764 |
|  | Control | 72.4 | 6.0 | – |

The data are shown in mm².



**Fig. 4.** Representative photomicrographs of tissue sections from each group at 1 week after surgery. (a, b) AD-T group; (c, d) GS group; and (e, f) control group. b, d, and f (×400) are higher magnification versions of a, c, and e (×40), respectively. The AD-T group showed granulation tissue formation composed of numerous fibroblasts and new blood vessels under blood clots (a, b). In addition, the appearance of cubic osteoblasts is confirmed on the bone surface (b: black arrow). In the GS group, the wound surface is covered with GS (c, d: *). In the control group, the wound surface is divided into a clot-covered area and an exposed bone area (e, f).

osteoblasts had appeared at the surface of the bone (Fig. 4b). In the GS group, the wound surface was covered with GS (Figs. 4c and 4d). In the control group, the wound surface was covered with blood clots in some parts and the bone was exposed in other parts (Figs. 4e and 4f).

At 2 weeks after surgery, the AD-T group showed granulation tissue formation composed of numerous fibroblasts and new blood vessels, as well as the presence of flat osteoblasts on the surface of the bone (Figs. 5a and 5b). In the GS group, the wound surface was covered with GS, but there was no granulation tissue formation (Figs. 5c and 5d). In the control group, findings were the same as those of the first week, namely, the wound surface was covered with blood clots in some parts and the bone was exposed in other parts (Figs. 5e and 5f).

At 4 weeks after surgery, complete epithelialization was found in the AD-T group (Figs. 6a and 6b). In the GS group, there were portions where GS was present, mixed with portions showing the formation of a granulation tissue composed of fibroblasts and newly formed

blood vessels (Figs. 6c and 6d). In the control group, there was still no epithelialization and the bone was still exposed (Figs. 6e and 6f).

Figure 7 shows microscopic images of the immuno-histochemistry findings of representative tissue sections in the AD-T group at 1 week after surgery. In this figure, the wounds are referred to as healing sites, whereas the healthy sites are referred to as normal sites.

Figures 7a and 7c show microscopic images of healing sites, whereas Figs. 7b and 7d show microscopic images of normal sites. Fibroblasts, newly formed capillaries, and osteoblasts in the healing sites reacted positively to anti-cortactin antibodies (Figs. 7a and 7c), whereas no positive reaction was observed in the connective tissue, normal vessels, or flat osteoblasts in the normal sites (Figs. 7b and 7d). Despite differences in the speed and effect of healing, immunohistochemical findings in the GS and control groups were similar to those in the AD-T group for the healing sites.
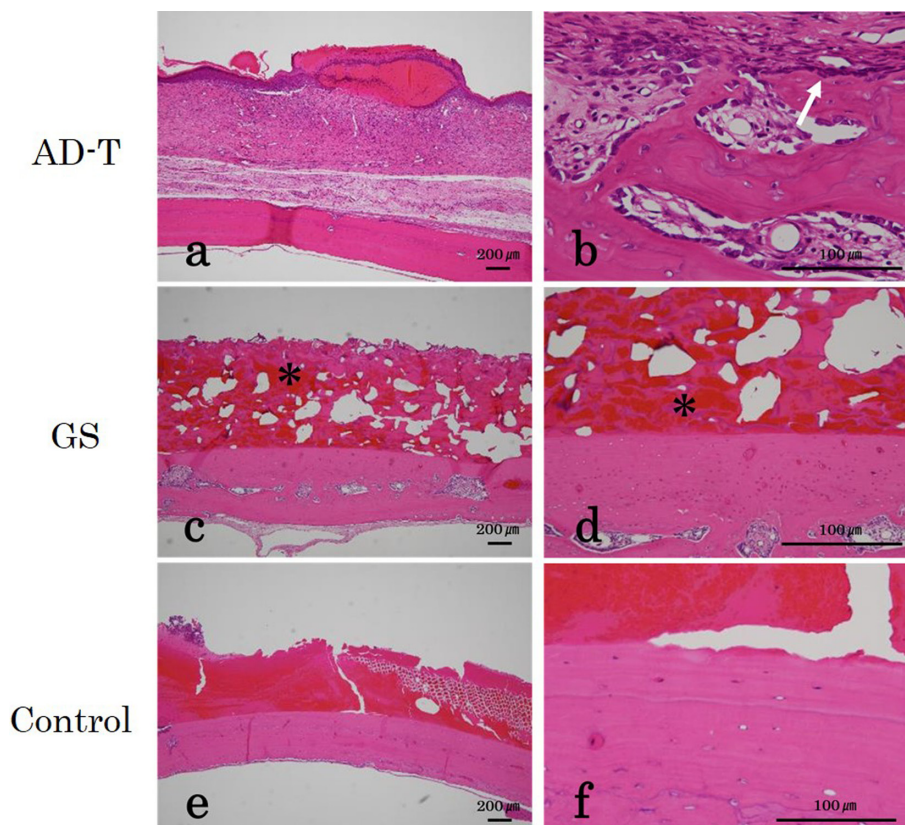


**Fig. 5.** Representative photomicrographs of tissue sections from each group at 2 weeks after surgery. (a, b) AD-T group; (c, d) GS group; and (e, f) control group. b, d, and f (×400) are higher magnification version of a, c, and e (×40), respectively. The appearance of flat osteoblasts on the bone surface is confirmed in addition to the formation of granulation tissue consisting of numerous fibroblasts and new blood vessels in the AD-T group (b: white arrow). In the GS group, the wound surface is covered with GS, but no granulation tissue formation can be observed (c, d: *). In the control group, the wound surface is divided into a clot-covered area and an exposed bone area (e, f).
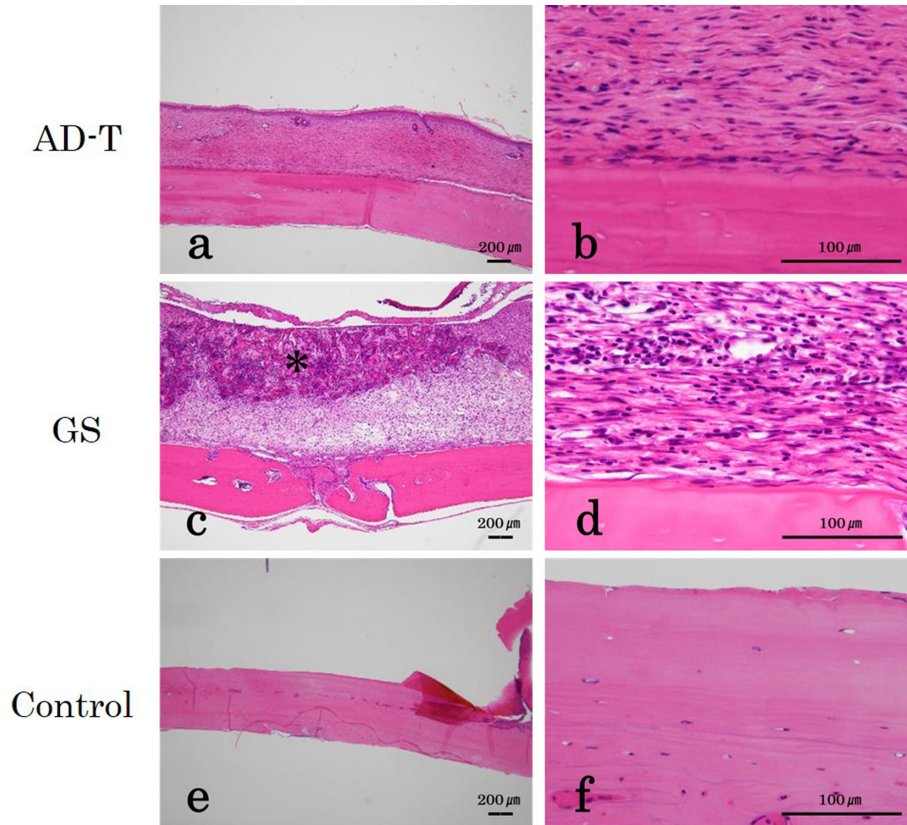
**Fig. 6.** Representative photomicrographs of tissue sections from each group at 4 weeks after surgery. (a, b) AD-T group; (c, d) GS group; and (e, f) control group. b, d, and f (×400) are higher magnification versions of a, c, and e (×40), respectively. Complete epithelialization is observed in the AD-T group (a, b). In the GS group, granulation tissue formation, including GS-remaining part, fibroblasts, and new blood vessels (c, d). In the control group, the bone remains exposed (e, f).
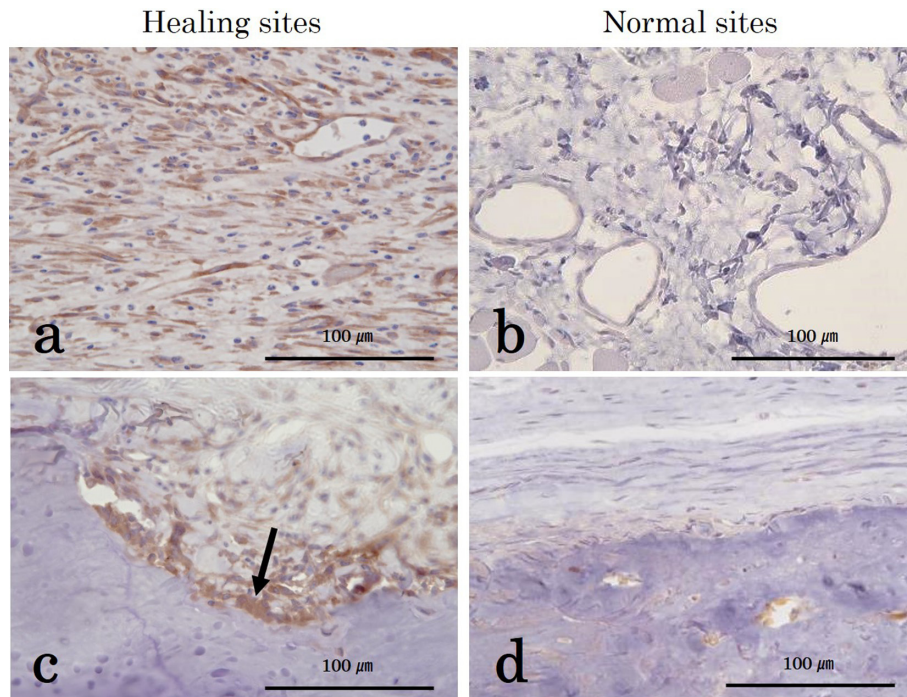


**Fig. 7.** Immunohistochemical staining of tissue sections in the AD-T group 1 week after surgery (a–d; × 400). Microscopic images of representative tissue sections in the AD-T group at 1 week after surgery; a and c show microscopic images of healing sites, whereas b and d show microscopic images of normal sites. Fibroblasts, newly developed capillaries, and cubic osteoblasts in the healing sites reacted positively to anti-cortactin antibodies (a, c, c; cubic osteoblasts, black arrow), whereas no positive reaction was observed at the normal sites (b, d).

## Quantitative analysis of cortactin-positive cells

Figure 8 shows the total number of cells and the proportion of cortactin-positive fibroblasts to in each group. The data are shown as mean ± SD.

At 1 week after surgery, the AD-T group had the highest total number of fibroblasts among the three groups, but it decreased from week 2 to week 4 after surgery. At 4 weeks after surgery, the GS group had the highest total number of fibroblasts among the three groups.

At 1 week after surgery, the AD-T group had the highest proportion of cortactin-positive fibroblasts among the three groups, but it decreased from week 2 to week 4 after surgery. At 4 weeks after surgery, the GS group had the highest proportion of cortactin-positive fibroblasts among the three groups.

Table 2 shows summary of measurements of the total number of fibroblasts and the proportion of cortactin-positive fibroblasts to the total number of fibroblasts at 1, 2, and 4 weeks after surgery.

At 1 week after surgery, in the total number of fibroblasts, the AD-T group was significantly different in comparison with the control group ($P<0.01$). At 4 weeks after surgery, the GS group was significantly different in comparison with the control group ($P<0.01$).

At 1 week after surgery, in the proportion of cortactin-positive fibroblasts to the total number of fibroblasts, the AD-T group was significantly different in comparison with the control group ($P<0.05$). At 4 weeks after surgery, the AD-T group was significantly different in comparison with the control group ($P<0.0001$).
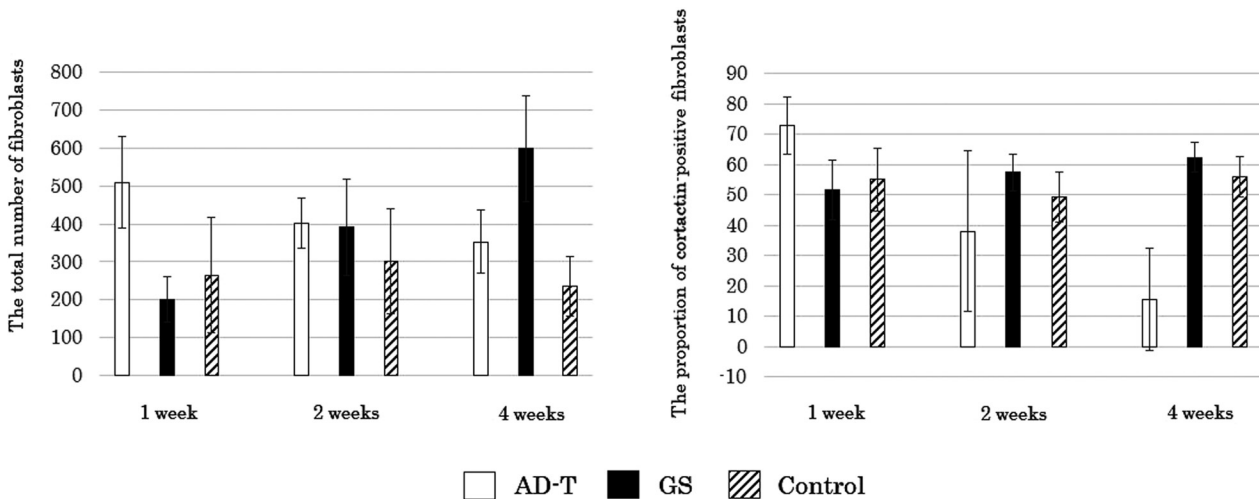


**Fig. 8.** The total number of fibroblasts and the proportion of cortactin-positive fibroblasts. At 1 week after surgery, the AD-T group had the highest total number of fibroblasts among the three groups, but it decreased from week 2 to week 4 after surgery. At 4 weeks after surgery, the GS group had the highest total number of fibroblasts among the three groups. At 1 week after surgery, the AD-T group had the highest proportion of cortactin-positive fibroblasts among the three groups, but it decreased from week 2 to week 4 after surgery. At 4 weeks after surgery, the GS group had the highest proportion of cortactin-positive fibroblasts among the three groups.

**Table 2.** Summary of measurements of the total number of fibroblasts and the proportion of cortactin-positive fibroblasts to the total number of fibroblasts

| | group | The total number of fibroblasts* | | | The proportion of cortactin-positive fibroblasts to the total number of fibroblasts** | | |
|---|---|---|---|---|---|---|---|
| | | mean | SD | *P*-value | mean | SD | *P*-value |
| 1 week after surgery | AD-T | 508.8 | 119.9 | <0.01 | 72.7 | 9.4 | <0.05 |
| | GS | 201.6 | 59.3 | 0.4074 | 51.8 | 9.8 | 0.6049 |
| | Control | 265.2 | 152.5 | – | 55.1 | 10.4 | – |
| 2 weeks after surgery | AD-T | 401.6 | 65.5 | 0.1892 | 38.0 | 26.5 | 0.2928 |
| | GS | 392.0 | 126.9 | 0.2317 | 57.5 | 6.1 | 0.4512 |
| | Control | 300.6 | 138.2 | – | 49.4 | 8.3 | – |
| 4 weeks after surgery | AD-T | 352.6 | 83.9 | 0.0982 | 15.5 | 16.8 | <0.0001 |
| | GS | 598.2 | 139.1 | <0.001 | 62.3 | 4.9 | 0.3768 |
| | Control | 234.6 | 78.0 | – | 56.1 | 6.6 | – |

*The data are shown in cells. **The data are shown in %.

## Cranial bone thickness

Figure 9 shows the bone thickness in each group. The data are shown as mean ± SD. Bone thickness had decreased in all groups at 2 weeks after surgery. In the AD-T group, bone thickness increased from week 2 to week 4 after surgery, whereas in the GS group and control group, bone thickness decreased continually from week 2 to week 4 after surgery. The greatest decrease in bone thickness was found in the control group.

Table 3 shows adjusted mean differences of the AD-T or GS group with the control group estimated with GEE, along with mean and SD in each group, for bone thickness at 1, 2, and 4 weeks after surgery. At 4 weeks after surgery, the AD-T group was significantly different in comparison with the control group ($P<0.0001$). For the comparison of straight lines, the AD-T group was significantly different in comparison with the control group ($P=0.0081$), whereas the GS group was not ($P=0.3614$).
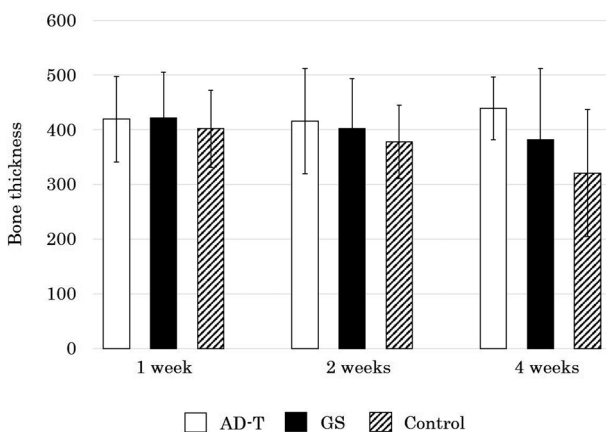


**Fig. 9.** Changes in cranial bone thickness. The postsurgical cranial bone thickness decreased in all groups from 1 week to 2 weeks. The cranial bone thickness increased from 2 weeks to 4 weeks after surgery in the AD-T group, whereas it decreased in the GS and control groups.

## Discussion

In the present study, a head wound with exposed bone surface was created in each of the rats, which were allocated to an AD-T group (treated by suturing AD-T onto the wound), GS group (treated by placing GS on the wound), and control group (in which the wound was left open). Comparisons between the groups showed that, macroscopically, wound healing was most accelerated in the AD-T group. After the first week following surgery, histopathological findings in the AD-T group showed a proliferation of anti-cortactin antibody-positive fibroblasts, a presence of newly formed blood vessels, as well as a proliferation of cubic osteoblasts. These findings indicated that AD-T was more suitable than GS as a wound dressing material.

We have used the same rat model as in this study to create head wounds with exposed bone; however, in our previous study, we covered the wounds with GS as well as PGA-FG and observed the progression of wound healing. Our findings showed that complete wound healing was achieved earlier in the group with the wound covered with GS than in the group with the wound covered with PGA-FG. GS is a water-insoluble hemostatic agent composed of bovine or porcine collagen [10]. It was first used as a surgical hemostatic agent in 1945. It is now commonly used to promote blood coagulation [11, 12]. GS has a hydrophilic structure and has been used as a scaffold for mesenchymal stem cells because of its absorptive capacity; GS has also been used as a medium for the controlled release of growth factors as well as for differentiation and induction factors [13, 14]. In the field of oral surgery, GS is mainly used for hemostasis of extraction sockets; therefore, the purpose of our study was to find dressing materials with better wound-healing efficacy than that of artificial dermis Terudermis® (AD-T), which has been used as a dressing material in actual clinical practice.

**Table 3.** Summary of measurements of the cranial bone thickness

| | group | mean | SD | adjusted mean difference | Robust S.E. | Robust Z | P-value |
|---|---|---|---|---|---|---|---|
| 1 week after surgery | AD-T | 419.5 | 78.6 | 17.7 | 33.2 | 0.53 | 0.5936 |
| | GS | 421.5 | 84.4 | 19.7 | 31.4 | 0.63 | 0.5312 |
| | Control | 401.8 | 71.1 | – | | | |
| 2 weeks after surgery | AD-T | 416 | 96.5 | 37.9 | 34.4 | 1.1 | 0.2713 |
| | GS | 402.1 | 91.8 | 24.0 | 26.3 | 0.91 | 0.3605 |
| | Control | 378.1 | 67.1 | – | | | |
| 4 weeks after surgery | AD-T | 439.2 | 57.4 | 118.4 | 24.0 | 4.94 | <0.0001 |
| | GS | 381.8 | 130.7 | 60.9 | 36.0 | 1.69 | 0.0909 |
| | Control | 320.8 | 116.6 | – | | | |

The data are shown in $\mu$m. Mean and SD in each group and adjusted mean differences of AD-T group or GS group with control group estimated using GEE for bone thickness at 1, 2, and 4 weeks after surgery.

AD-T is a dermal defect graft in which a silicon film has been added to the upper part of an artificial dermis made from processed atelocollagen in order to prevent exogenous infection and adjust permeability to exudates [15]. Atelocollagen, the raw material of AD-T, is a bovine dermis-derived type I collagen, which has a rod-shaped molecule (300 nm in length and 1.5 nm in width) in which three polypeptide chains with repeated sequences of Gly-Pro-Hyp amino acids form a helix; the molecule has non-helical telopeptides at both terminal ends [16]. The antigenicity of collagen is mainly because of the telopeptides, and atelocollagen is the product of the digestion and cleavage of those telopeptides by proteases; this is why atelocollagen is a protein with extremely low antigenicity [16]. The mechanism behind the effect of AD-T is that when AD-T is applied to a full-thickness skin defect wound, capillaries and fibroblasts from the bed and margins of the wound penetrate the pores of the collagen sponge [17]. The invading capillaries extend toward the central and upper layers of the collagen sponge while branching out to form a vascular network [17]. Fibroblasts also grow and spread from the middle layers to the upper layers of the collagen sponge [17]. As for the cross-sectional morphology of AD-T, a sponge-like multilayered structure has been found in scanning electron micrographs [18], suggesting that it may serve as a scaffold that facilitates the penetration of capillaries and fibroblasts which are necessary for wound healing. While the collagen sponge is gradually decomposed and absorbed, new collagen is produced by the proliferating fibroblasts and is replaced by a new dermis-like tissue in 2 to 3 weeks [17]. AD-T has shown excellent clinical outcomes not only in skin defect wounds but also in oral mucosal defects [15, 17, 19–22]. Furthermore, since the silicon membrane attached to AD-T is processed using a polyester mesh, it can be sutured and fixed to the surrounding tissue [20]. In this study, immunohistochemical staining showed that in the AD-T group, fibroblasts, capillary endothelial cells, and cubic osteoblasts in the healing sites displayed a positive reaction to anti-cortactin antibodies whereas normal sites did not. Cortactin is an F-actin-binding protein localized at the cell margin where actin remodeling occurs to allow for cell migration [23]. Remodeling of the actin cytoskeleton affects cell migration, motility, and adhesion, as well as tumor invasion and metastasis [24]. Cortactin also controls the dynamic actin network underlying lamellipodia expansion and cell dispersion, thus allowing cells to rapidly coat the wound and contribute to wound healing [9]. In addition, type I collagen is known to induce F-actin organization on endothelial cells, macrophages, fibroblasts, as well as tumor cells [25], and in

the presence of atelocollagen from type I collagen, cortactin-positive fibroblasts and newly developing capillaries are more likely to assemble, allowing for early wound healing.

Previous reports suggest that fibroblasts, which play a major role in wound healing, are dominant during granulation tissue formation, but undergo apoptosis and decline as wound healing is completed [26, 27].

In the present study, at 1 week after surgery, the AD-T group had the highest total number of fibroblasts and had the highest proportion of cortactin-positive fibroblasts among the three groups, but they decreased from week 2 to week 4 after surgery. These findings suggested that the AD-T group showed a faster progression of postoperative wound healing than the other groups, and wound healing seemed to be completed in a shorter period of time.

Regarding bone thickness, in this study, the periosteum was removed along with the skin in order to create wounds with exposed bone on the rats' heads. The periosteum is a fibrous, highly angiogenic panniculus which tightly adheres to a bone's outer surface [28]. Histologically, the periosteum can be divided into a deep layer in contact with the bone (cambium layer) and a superficial fibrous layer (stratum fibrosum) [28]. The former contains a high density of osteoblasts and preosteoblasts, and the latter contains fibroblasts [28]. The periosteum is involved in bone formation and supplies blood to the cortical bone [29, 30]. Furthermore, periosteum-derived bone formation also involves periosteal cells which are released from the cambium and differentiate into free osteoblasts [31].

Osteoblasts form the organic matrix of the bone and are also involved in bone calcification as well as in the induction of osteoclast differentiation. Osteoblasts are arranged in a single layer, like epithelial cells, on the bone formation surface. When bone formation is active, osteoblasts take a cuboidal or fusiform shape, and the nucleus is ubiquitous with a single prominent nucleolus. Under conditions of reduced bone formation, osteoblasts become flattened and ultimately remain as a cellular lining of the bone surfaces [32]. Large bone defects and the removal of periosteum along with the exposure of bone often pose a high risk of bacterial infection. Bacteria induce apoptosis of osteoblasts, resulting in bone destruction [33]. In order to avoid delayed wound healing resulting from infection, wound dressings that allow bone as well as soft tissue to heal are necessary. In this study, the periosteum involved in bone formation was removed, but in the AD-T group, cubic osteoblasts started appearing on the bone surface at 1 week after surgery; this became a mixture of cubic and flat osteo-

blasts at 2 weeks after surgery; osteoblasts disappeared at four weeks after surgery, resulting in an increased bone thickness. By contrast, in the control and GS groups, bone thickness remained low even in the fourth week after surgery. Because atelocollagen helps with osteoblast migration, proliferation, and growth [34], it is considered more suitable than GS as a wound dressing material for the treatment of wounds with bone defects.

In this study, the AD-T group showed no obvious scar contracture in the wound area, and good healing was achieved. The findings were similar to those of two other studies in which AD-T was applied to rat palatal gingival defects [17, 35]. However, scar contracture has been reported to be present in cases where the area of the defect is large [2]. The present study results suggest that AD-T is useful in the clinical setting, where large wounds are expected, and suturing can be performed to prevent the material from falling out. In the future, the wound-healing efficacy of other additional wound dressing materials will need to be investigated in larger animal models.

## Conclusions

AD-T facilitated the aggregation of cortactin-positive fibroblasts and vascular endothelial cells and promoted the migration and growth of osteoblasts, which helped achieve early wound healing. Therefore, in the treatment of wounds with bone defects, AD-T can be considered as a more suitable wound dressing material than GS.

## Acknowledgments

## References

1. Tsuno H, Arai N, Sakai C, Okabe M, Koike C, Yoshida T, et al. Intraoral application of hyperdry amniotic membrane to surgically exposed bone surface. Oral Surg Oral Med Oral Pathol Oral Radiol. 2014; 117: e83–e87. [Medline] [CrossRef]

2. Murata M, Umeda M, Takeuchi J, Suzuki H, Shibuya Y, Shigeta T, et al. Application of polyglycolic acid sheet (Neoveil®) and fibrin glue spray (Bolheal®) for open wounds in oral surgery. J Jpn Stomatol Soc. 2011; 60: 232–239.

3. Kaneda T, Shibata S, Nagayama M. Clinical application of flexible fibrin film in oral surgery. Jpn J Oral Maxillofac Surg. 1973; 19: 357–364. [CrossRef]

4. Kondoh T, Kikuta T, Kinebuchi T, Takarada H. Clinical application of lyophilized porcine skin in the oral region. Jpn J Oral Maxillofac Surg. 1980; 26: 1128–1134. [CrossRef]

5. Hall HD, O'Steen AN. Free grafts of palatal mucosa in mandibular vestibuloplasty. J Oral Surg. 1970; 28: 565–574. [Medline]

6. Ohtsuki K, Ohnishi M, Nakamura Y, Kurokawa E. Clinical application of "Chitin", artificial skin material in oral mucous defects. Jpn J Oral Maxillofac Surg. 1990; 36: 2103–2110. [CrossRef]

7. Paddle-Ledinek JE, Nasa Z, Cleland HJ. Effect of different wound dressings on cell viability and proliferation. Plast Reconstr Surg. 2006; 117:(Suppl): 110S–118S, discussion 119S–120S. [Medline] [CrossRef]

8. Koshinuma S, Murakami S, Noi M, Murakami T, Mukaisho KI, Sugihara H, et al. Comparison of the wound healing efficacy of polyglycolic acid sheets with fibrin glue and gelatin sponge dressings in a rat cranial periosteal defect model. Exp Anim. 2016; 65: 473–483. [Medline] [CrossRef]

9. Choi S, Camp SM, Dan A, Garcia JG, Dudek SM, Leckband DE. A genetic variant of cortactin linked to acute lung injury impairs lamellipodia dynamics and endothelial wound healing. Am J Physiol Lung Cell Mol Physiol. 2015; 309: L983–L994. [Medline] [CrossRef]

10. Loffroy R, Guiu B, Cercueil JP, Krausé D. Endovascular therapeutic embolisation: an overview of occluding agents and their effects on embolised tissues. Curr Vasc Pharmacol. 2009; 7: 250–263. [Medline] [CrossRef]

11. Jenkins HP, Janda R. Studies on the use of gelatin sponge or foam as an hemostatic agent in experimental liver resections and injuries to large veins. Ann Surg. 1946; 124: 952–961. [CrossRef]

12. Evans BE. Local hemostatic agents. N Y J Dent. 1977; 47: 109–114. [Medline]

13. Kim JC, Choi SS, Wang SJ, Kim SG. Minor complications after mandibular third molar surgery: type, incidence, and possible prevention. Oral Surg Oral Med Oral Pathol Oral Radiol Endod. 2006; 102: e4–e11. [Medline] [CrossRef]

14. Omata K, Matsuno T, Asano K, Hashimoto Y, Tabata Y, Satoh T. Enhanced bone regeneration by gelatin-β-tricalcium phosphate composites enabling controlled release of bFGF. J Tissue Eng Regen Med. 2014; 8: 604–611. [Medline] [CrossRef]

15. Goto H, Higa E, Kanbara M, Haraga I. Our experience using artificial skin grafts arising from calf skin and collagen. Orthop Traumatol. 1998; 47: 679–684. [CrossRef]

16. Makita N, Nagahara S. Recent progress of nucleic acid delivery system mediated by atelocollagen. Drug Deliv Syst. 2010; 25: 607–614. [CrossRef]

17. Suzuki S. Artificial dermis as a medical material for regenerative medicine-from the past to present. Plast Surg (Oakv). 2018; 61: 389–399.

18. Minabe M, Sato J, Sekino S, Okamoto H. Basic studies on wound healing responses after collagen matrix implantation into defects of the palatal gingiva of rats. Jpn J Conserv Dent. 1993; 36: 894–901.

19. Kawabe R, Mizuki N, Usui S, Saito T, Miyazaki C, Horimoto S, et al. Clinical evaluation of a new collagen sponge and silicone bilayer "artificial mucous membrane" for the resection of oral tumors. Head Neck Cancer. 1995; 21: 219–223. [CrossRef]

20. Fushimi H, Kodama T, Tsutsumi K, Kitsugi D, Sugiyama T, Ikai H, et al. The effect of artificial dermis (Terudermis®) applied to muco-gingival surgery. J Jpn Soc Oral Implant. 1997; 10: 45–54.

21. Shirai Y, Bessho K, Nishida M, Murakami K, Iizuka T. The usefulness of a bilayer artificial dermis (Terudermis®) for vestibular extension in the mandible. Jpn J Oral Maxillofac Surg. 1995; 41: 896–898. [CrossRef]

22. Mizuki N, Omura S, Aoki S, Umino S, Kawabe R, Ishikawa Y, et al. Clinical evaluation of a new collagen sponge and silicone bilayer "artificial mucous membrane" for the repair of oral mucosal defects. Jpn J Oral Maxillofac Surg. 1994; 40: 776–784. [CrossRef]

23. Noi M, Mukaisho KI, Yoshida S, Murakami S, Koshinuma S, Adachi T, et al. ERK phosphorylation functions in invadopodia formation in tongue cancer cells in a novel silicate

fibre-based 3D cell culture system. Int J Oral Sci. 2018; 10: 30. [Medline] [CrossRef]

24. Folio C, Zalacain M, Zandueta C, Ormazábal C, Sierrasesúmaga L, San Julián M, et al. Cortactin (CTTN) overexpression in osteosarcoma correlates with advanced stage and reduced survival. Cancer Biomark. 2011-2012; 10: 35–41. [Medline] [CrossRef]

25. Juin A, Billottet C, Moreau V, Destaing O, Albiges-Rizo C, Rosenbaum J, et al. Physiological type I collagen organization induces the formation of a novel class of linear invadosomes. Mol Biol Cell. 2012; 23: 297–309. [Medline] [CrossRef]

26. Reinke JM, Sorg H. Wound repair and regeneration. Eur Surg Res. 2012; 49: 35–43. [Medline] [CrossRef]

27. Hinz B. Formation and function of the myofibroblast during tissue repair. J Invest Dermatol. 2007; 127: 526–537. [Medline] [CrossRef]

28. Landry PS, Marino AA, Sadasivan KK, Albright JA. Effect of soft-tissue trauma on the early periosteal response of bone to injury. J Trauma. 2000; 48: 479–483. [Medline] [CrossRef]

29. Kowalski MJ, Schemitsch EH, Kregor PJ, Senft D, Swiontkowski MF. Effect of periosteal stripping on cortical bone perfusion: a laser doppler study in sheep. Calcif Tissue Int. 1996; 59: 24–26. [Medline] [CrossRef]

30. Rücker M, Binger T, Deltcheva K, Menger MD. Reduction of midfacial periosteal perfusion failure by subperiosteal versus supraperiosteal dissection. J Oral Maxillofac Surg. 2005; 63: 87–92. [Medline] [CrossRef]

31. Iuchi T. Comparative study of impact on osteogenesis and chondrogenesis in tissue-engineered phalanx between different periostea. Med J Kindai Univ. 2018; 43: 117–126.

32. Stacey E, Mills MD. Bone-the tissue: organic and inorganic components. In: Histology for pathologists 5th ed., Philadelphia: Wolters Kluwer; 2020. pp. 96–98.

33. Arciola CR, Campoccia D, Montanaro L. Implant infections: adhesion, biofilm formation and immune evasion. Nat Rev Microbiol. 2018; 16: 397–409. [Medline] [CrossRef]

34. Suh H, Hwang YS, Lee JE, Han CD, Park JC. Behavior of osteoblasts on a type I atelocollagen grafted ozone oxidized poly L-lactic acid membrane. Biomaterials. 2001; 22: 219–230. [Medline] [CrossRef]

35. Kodama T, Tsutsumi K, Fushimi H, Fuchida T, Hori T, Ozono S, et al. Application of artificial dermis to periodontal therapy-Epithelial regeneration responses after collagen matrix implantation into defects of the palatal gingiva in rats. J Jpn Soc Periodontol. 1994; 36: 162–169. [CrossRef]